

Combined AFM–Confocal Microscopy of Oil Droplets: Absolute Separations and Forces in Nanofilms

Rico F. Tabor,^{†,‡} Hannah Lockie,^{†,‡} Douglas Mair,[§] Rogerio Manica,[⊥] Derek Y. C. Chan,^{‡,#,∇} Franz Grieser,^{‡,¶} and Raymond R. Dagastine^{*,†,‡}

[†]Department of Chemical and Biomolecular Engineering, [‡]Particulate Fluids Processing Centre, [#]Department of Mathematics and Statistics, and [¶]School of Chemistry, University of Melbourne, Parkville 3010, Australia

[§]Melbourne Centre for Nanofabrication, 151 Wellington Road, Clayton 3168, Australia

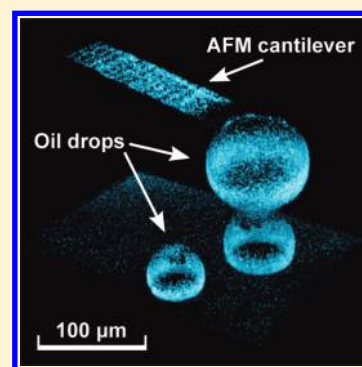
[⊥]Institute of High Performance Computing, 138632, Singapore

[∇]Faculty of Life and Social Science, Swinburne University of Technology, Hawthorne 3122, Australia

S Supporting Information

ABSTRACT: Quantitative interpretation of the dynamic forces between micrometer-sized deformable droplets and bubbles has previously been limited by the lack of an independent measurement of their absolute separation. Here, we use in situ confocal fluorescence microscopy to directly image the position and separation of oil droplets in an atomic force microscopy experiment. Comparison with predicted force vs. separation behavior to describe the interplay of force and deformation showed excellent agreement with continuum hydrodynamic lubrication theory in aqueous films less than 30 nm thick. The combination of force measurement and 3D visualization of geometric separation and surface deformation is applicable to interactions between other deformable bodies.

SECTION: Macromolecules, Soft Matter



Understanding the interactions between drops and bubbles requires a detailed knowledge of the nanoscale spatial variations of the liquid films between these types of deformable objects. This is important in established processing areas such as personal care products, food technology, and pharmaceutical purification and also in more recent innovations such as micro- and nanofluidic devices where drops and bubbles are vectors for transport, mixing, and synthesis of materials.^{1,2} It is therefore vital to develop a quantitative understanding of how such micrometer-scale deformable bodies such as drops and bubbles interact with one another, and with solid surfaces, at nanometer separations.³ As a droplet approaches a surface, it deforms in response to the hydrodynamic⁴ and colloidal⁵ or surface forces⁶ acting in the film of intervening liquid. Such complex coupling between forces and geometry dictate stability and coalescence in emulsions and foams and is critical in microfluidic devices as well, where this interplay between deformation and force controls droplet motion and friction/lubrication in channels and determines whether coalescence will occur during interaction events.^{7,8}

To quantify these processes, accurate knowledge of three elements is required: the position of the drops or bubbles, the forces acting between them, and the profile of the intervening nanoscale liquid films.⁹ The atomic force microscope (AFM) represents the ideal tool for measuring forces between droplets, to sub-nano-Newton resolution.⁴ The relative position of the

drops or bubbles can be controlled through surface immobilization in aqueous solution by carefully manipulating the contact angles of the cantilever and substrate.¹⁰ Additionally, custom-designed AFM cantilevers allow for subnanometer positioning of the drops or bubbles and provide well-defined contact geometries.¹¹ What is lacking in conventional AFM experiments is a quantitative measure of the separation between the surfaces, which ranges from a few micrometers down to a few nanometers. For interactions between solid objects such as particles and hard surfaces, the absolute separation between the interacting surfaces at all times can be known by calibrating against the point of hard contact¹² and has been measured independently with evanescent wave scattering.¹³ However, for objects such as droplets that can deform, determining the absolute separation is more complex as contact may never occur, and both the droplet and cantilever can deform in response to separation- and velocity-dependent surface and hydrodynamic forces.¹⁴ Hence, an independent measure of absolute separation is vital in order to analyze these systems.

Previous approaches to measuring the separation between larger deformable surfaces have relied on optical interferometry.^{15,16} However, when moving to emulsion droplets, this technique is

Received: March 16, 2011

Accepted: April 6, 2011

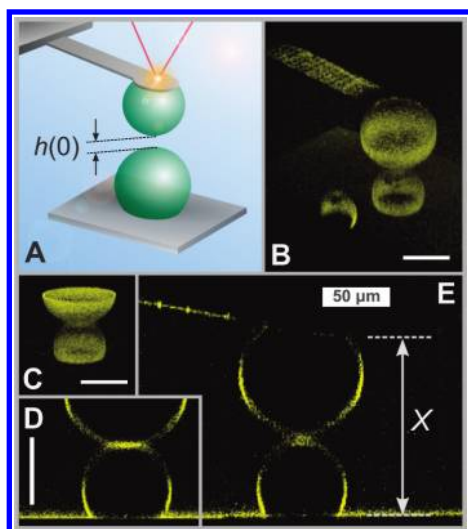


Figure 1. (A) Schematic of the experimental setup, showing an oil drop captured on the AFM cantilever, positioned over a surface-immobilized drop in an aqueous dye solution. (B) 3D confocal image of two drops before an interaction event. (C) 3D confocal image of the same two drops during an interaction at a high force loading, where the drops deform to give a region of flat film. (D) Vertical (YZ) slice of the two deformed drops shown in (C). (E) Vertical (YZ) slice of the same two drops at a separation of $8\ \mu\text{m}$. The white rectangle in each image is a scale bar representing $50\ \mu\text{m}$.

quite limited because of the small lateral dimensions available. Additionally, a large difference in the refractive index of the drop phase and continuous phase is needed to ensure high optical precision. This may not be possible for common water/oil systems.

In this study, we use laser scanning confocal fluorescence microscopy to measure the absolute separation between droplets in situ in an AFM experiment and also to quantify deformations in the nanofilm region during interactions. An advantage of confocal fluorescence microscopy is that, unlike interferometry, it does not require curved interfaces, and hence, the flat films generated between interacting objects that are “invisible” to interferometry can be seen. To demonstrate the effectiveness of the technique and the accuracy of the comparison between AFM force data and confocal images, measurements of absolute separations for rigid systems were first made by both methods and compared (see Supporting Information).

Confocal microscopy has grown to prominence as a tool for analyzing biological systems¹⁷ as internal components of cells can be readily visualized in three spatial dimensions and noninvasively by staining with fluorescent dyes or labels. More recently, it has started to become an important tool for understanding colloidal systems such as vesicles.¹⁸ Previous combined AFM/confocal studies have focused on observing the effects of an applied force during biological processes,¹⁹ such as cell death²⁰ and fiber growth.²¹

Full details of materials and experimental methods are contained in Supporting Information. Briefly, droplets of perfluorooctane (PFO) were generated using a syringe to disperse the oil under water in a specially made fluid cell. This fluorinated oil was selected as the droplet phase in these experiments because of its density ($1.77\ \text{g}/\text{cm}^3$), refractive index (1.30, slightly below that of water, 1.33), and desirable chemical characteristics,²² including

vanishing water solubility, ensuring stable drops with a well-defined oil/water interface. A PFO droplet was then captured on the cantilever of the AFM, which was mounted on an inverted confocal microscope, to provide the necessary bottom-up geometry. An Acid Red 88 solution was added to act as the fluorescent dye; this molecule adsorbed to both the solid–water and oil–water interfaces in the system. The cantilever and drop were then positioned above another surface-immobilized drop to measure drop–drop interactions (Figure 1A) or over an area of surface where no drops were immobilized to measure drop–surface interactions. A confocal image was obtained, and an interaction event was measured with the AFM immediately afterward. Confocal images were used to find the precise location of the droplet interfaces (Figure 1D,E) and hence determine their separation to within 50 nm.

In order to validate the effectiveness of confocal imaging for measuring absolute separations in the AFM experiment, an image of the cantilever a few micrometers from the surface was taken. The AFM was then used to bring the cantilever down until it contacted the solid substrate. The distance traveled by the AFM cantilever, as measured by the sensor of the AFM, was then compared to the initial separation determined from the confocal image. The two independent measurements agreed to within 50 nm.

When dealing with droplets in confocal microscopy, it is clear from Figure 1 that there is a “lensing” effect due to refraction of light as it passes through the droplet interfaces in the confocal image. However, this is minimal because of the similar refractive indices of PFO and water, although it does mean that only certain parts of the drop profile could be used for accurate fitting of the drop shape. Due to the inverted geometry of the confocal microscope, any part of the drop that is directly “seen” in a vertical path from the bottom surface without having passed through a liquid–liquid interface is undistorted,¹⁷ and spherical fitting confirms this. Furthermore, transmission optical microscopy measurements were also used to confirm droplet diameters. It is envisaged that the lensing problem could be entirely avoided by using a mixture of perfluorobenzene (refractive index 1.38) and PFO as the droplet phase in order to match the refractive index of the oil to that of water. This would be more useful in obtaining full film profiles of distorted drops, particularly in circumstances where the film may be inhomogeneous due to, for example, particle adsorption.

Drop interface profiles were extracted by measuring the pixel intensity profiles of XY slices parallel to the surface at regular height steps through the two drops (Figure 2A,B). The position of the interface was taken as the maximum intensity point in the perimeter of the 2D circle (Figure 2C). Data were fitted for regions of the drops not affected by lensing of the interfaces. By fitting the profiles of the drops to circles, the relative position or separation of the two drops can be determined to a much higher accuracy than the spatial resolution that corresponds to a single pixel (see Supporting Information).

In order to analyze the deformational behavior of the droplets and hence that of the nanoconfined water film between them, a model based on hydrodynamic lubrication theory for flow in the thin film and the Young–Laplace equation to describe drop deformations was used to generate predicted force curves for comparison.²³ This model has been described previously in considerable detail^{9,23} and applied in order to analyze systems comprised of two deformable drops,⁴ a deformable bubble against a solid surface,^{11,24,25} and two bubbles.^{6,26} Time and

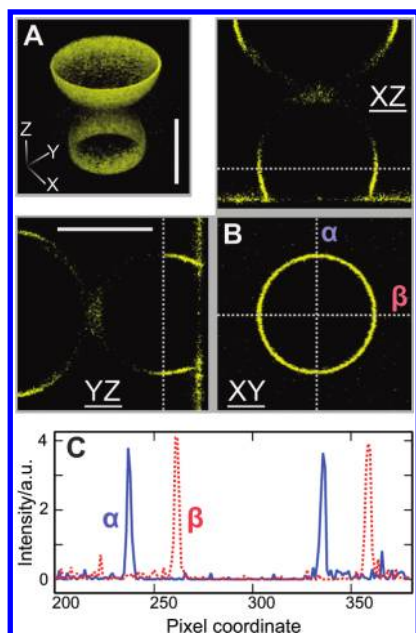


Figure 2. (A) 3D confocal image of two drops at a separation of $8 \mu\text{m}$. (B) XY, XZ, and YZ slices from the 3D confocal image in (A), taken at the points shown by gray dashed lines. (C) Intensity profiles of the slices measured along lines α and β , where one pixel corresponds to 630 nm . The white rectangle in each image is a scale bar representing $50 \mu\text{m}$.

spatial variations of deformations of the drops and the thickness of the nanofilm between the drops due to the hydrodynamic pressure and surface forces were calculated explicitly to determine variations of the cantilever deflection and hence the force of interaction as the drops were driven together or separated. Significantly, the model has no “free” parameters when the initial separation determined from confocal microscopy is available here as an input parameter. In previous studies, the absolute initial separation between the central point of the interfaces, $h(0)_{\text{initial}}$, was unknown and hence was unconstrained during fitting. By measuring this initial separation directly with confocal imaging, not only does this give direct information on the interfaces of the interacting bodies, but it also confirms the robustness of the theoretical framework.

Hence, confocal imaging was used to provide an independent measurement of the droplet separation before interaction (inset to Figure 3). The close agreement between the initial separation derived from theoretical modeling, $h(0)_{\text{initial}}^{\text{theory}}$, and the confocal image, $h(0)_{\text{initial}}^{\text{confocal}}$, suggests that the deformation of the interfaces when the drops interact is predicted accurately by the theoretical framework. We can therefore be confident that continuum hydrodynamics is obeyed for the films observed in this experiment.

Figure 3 shows the interaction between two oil droplets as they are brought together and then moved apart at a nominal speed of $45 \mu\text{m/s}$. As the AFM’s piezo drive is used to actuate the approach of the droplets (moving from right to left on the graph), there is a region where no interaction is experienced when the droplets are far apart and the film between them is several micrometers thick (a), and then, the force begins to increase (b). This is because the liquid between the drops as they approach offers some hydrodynamic resistance as the droplets are squeezed together. Once the film has thinned substantially (to $< \sim 100 \text{ nm}$), the force then increases rapidly, and the variation is not sensitive to the drive velocity (c), where the

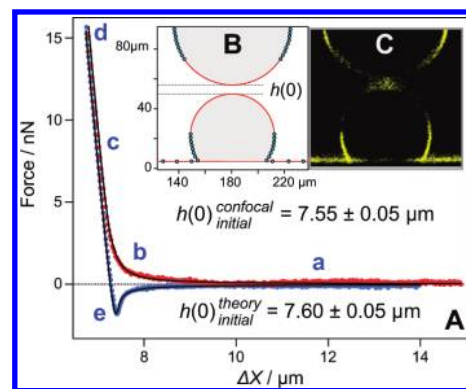


Figure 3. (A) Variation of the interaction force with relative displacement between two oil droplets at a nominal approach/retract speed of $45 \mu\text{m/s}$ measured with AFM. Colored markers are approach (red) and retract (blue) data, and solid lines are predictions from theoretical modeling. (B) Fitted profile from the confocal image used to obtain $h(0)_{\text{initial}}^{\text{confocal}}$. Note that for clarity, every the fifth data point is plotted. (C) Confocal image taken directly before the AFM measurement.

increasing Laplace pressure from deformation of the droplets contributes. The piezo drive is then used to retract the droplets when a fixed force of 16 nN has been reached (d). Upon retraction, a region of negative force is seen (e), corresponding to the hydrodynamic “suction” between the two droplets. Because of their highly charged surfaces (zeta potentials for the droplets were measured to be $-80 \pm 5 \text{ mV}$), the repulsive pressure in the water film between drops from electrical double-layer interactions was sufficient to maintain a continuous film at all points and inhibit coalescence between the drops (or between the drop and surface).

A similar interaction to the two-drop case is seen when a droplet interacts with a flat surface (Figure 4). However, due to the different geometry, the magnitude of the negative suction force experienced during retraction is greater. By visualizing the force in terms of film thickness (Figure 4A), it is clear that beyond a certain point, increasing the force acting on the droplet does not significantly thin the film. This is because the pressure from surface forces (in this case, a strong repulsion from overlap of electrical double layers) is greater than the Laplace pressure required to deform the droplet. The minimal film thickness (28 nm) is actually experienced upon retraction, where the dynamic suction effect of trying to separate the interfaces causes a negative hydrodynamic pressure, thinning the film by around 2 nm more than is achieved by the applied force. This is clearly velocity-dependent, with greater retract velocities expected to cause greater suction. This scenario is particularly relevant to microfluidics, where the interaction of droplets with channel walls is crucial. In this case, a continuous water film is preserved, suggesting that stable lubrication would be obtained at this interaction speed. These results aid in quantifying the role of dynamic forces and film drainage with relation to the surface forces acting between the solid–liquid and liquid–liquid interfaces.

An important strength of confocal microscopy is that because it relies on a fluorescence signal rather than reflection at interfaces, planar (flat) films can be observed. Figure 1C and D shows an interaction between two droplets at an applied force of 70 nN . From modeling, the film here is predicted to be only 30 nm thick and $\sim 10 \mu\text{m}$ in diameter. It is clear that direct visualization of this film would prove vital in circumstances where, for example, nanoparticles were adsorbed at the interfaces of the droplets.

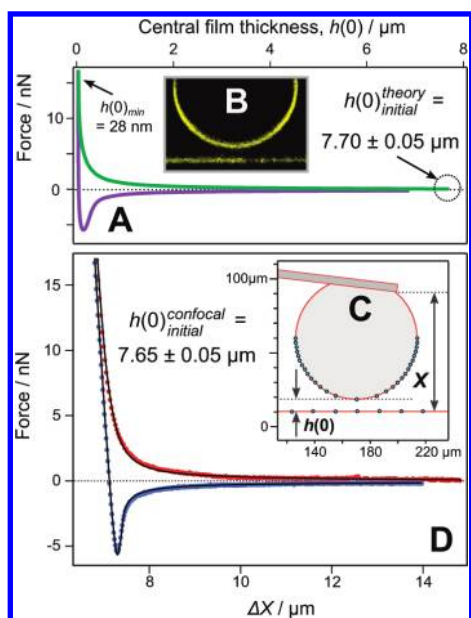


Figure 4. (A) Variation of the interaction force with relative displacement between an oil droplet and solid surface at a nominal approach/retract speed of $25 \mu\text{m/s}$ measured with AFM, shown as a function of the modeled central film thickness, $h(0)$. (B) Confocal image taken directly before the AFM measurement. (C) Fitted profile from the confocal image used to obtain $h(0)_{\text{confocal}}^{\text{initial}}$. Note that for clarity, every 10th data point is plotted. (D) Force interaction data as displayed in (A) but plotted as a function of the (measured) change in the cantilever–surface separation, ΔX . Colored markers are approach (red) and retract (blue) data, and solid lines are predictions from theoretical modeling.

In summary, a combined atomic force and laser scanning confocal microscope was used to analyze the interactions between, and spatial positioning of, oil droplets. It is seen that a continuum hydrodynamic model accurately describes the behavior of water films down to separations of tens of nanometers. Significantly, confocal imaging will prove to be a vital tool in the next generation of force experiments with more complex systems as it can be used where both continuum hydrodynamic theories and interferometric techniques for measuring separations break down. Examples may include particle-decorated interfaces, non-Newtonian fluids, index-matched systems, and nonhomogeneous adsorption at interfaces.

■ ASSOCIATED CONTENT

S Supporting Information. Details of experimental procedures and materials. This material is available free of charge via the Internet at <http://pubs.acs.org>.

■ AUTHOR INFORMATION

Corresponding Author

*E-mail: rrd@unimelb.edu.au.

■ ACKNOWLEDGMENT

X. S. Tang and S. O'Shea are thanked for preparing the cantilevers used. The ARC is thanked for financial support, and the Particulate Fluids Processing Centre provided infrastructure support for the project. This work was performed in part at the

Melbourne Centre for Nanofabrication, which is the Victorian node of the Australian National Fabrication Facility, an initiative partly funded by the Commonwealth of Australia and the Victorian Government.

■ REFERENCES

- (1) Teh, S.-Y.; Lin, R.; Hung, L.-H.; Lee, A. P. Droplet Microfluidics. *Lab Chip* **2008**, *8*, 198–220.
- (2) Duraiswamy, S.; Khan, S. A. Plasmonic Nanoshell Synthesis in Microfluidic Composite Foams. *Nano Lett.* **2010**, *10*, 3757–3763.
- (3) Baroud, C.; Gallaire, F.; Dangla, R. Dynamics of Microfluidic Droplets. *Lab Chip* **2010**, *10*, 2032–2045.
- (4) Dagastine, R. R.; Manica, R.; Carnie, S. L.; Chan, D. Y. C.; Stevens, G. W.; Grieser, F. Dynamic Forces Between Two Deformable Oil Droplets in Water. *Science* **2006**, *313*, 210–213.
- (5) Tabor, R. F.; Chan, D. Y. C.; Grieser, F.; Dagastine, R. R. Structural Forces in Soft Matter Systems. *J. Phys. Chem. Lett.* **2011**, *2*, 434–437.
- (6) Tabor, R. F.; Chan, D. Y. C.; Grieser, F.; Dagastine, R. R. Anomalous Stability of Carbon Dioxide in pH-Controlled Bubble Coalescence. *Angew. Chem., Int. Ed.* **2011**, *50*, 3454–3456.
- (7) Gunes, Z. D.; Clain, X.; Breton, O.; Mayor, G.; Burbidge, A. Avalanches of Coalescence Events and Local Extensional Flows — Stabilisation or Destabilisation Due to Surfactant. *J. Colloid Interface Sci.* **2010**, *343*, 79–86.
- (8) Tan, Y.-C.; Ho, Y. L.; Lee, A. P. Droplet Coalescence by Geometrically Mediated Flow in Microfluidic Channels. *Microfluid. Nanofluid.* **2007**, *3*, 495–499.
- (9) Chan, D. Y. C.; Manica, R.; Klaseboer, E. Film Drainage and Coalescence between Deformable Drops and Bubbles. *Soft Matter* **2011**, *7*, 2235–2264.
- (10) Lockie, H. E.; Manica, R.; Stevens, G. W.; Grieser, F.; Chan, D. Y. C.; Dagastine, R. R. Precision AFM Measurements of Dynamic Interactions between Deformable Drops in Aqueous Surfactant and Surfactant-Free Solutions. *Langmuir* **2011**, *27*, 2676–2685.
- (11) Manor, O.; Vakarelski, I. U.; Tang, X.; O'Shea, S. J.; Stevens, G. W.; Grieser, F.; Dagastine, R. R.; Chan, D. Y. C. Hydrodynamic Boundary Conditions and Dynamic Forces between Bubbles and Surfaces. *Phys. Rev. Lett.* **2008**, *101*, 024501/1–024501/4.
- (12) Smith, J. A.; Werzer, O.; Webber, G. B.; Warr, G. G.; Atkin, R. Surprising Particle Stability and Rapid Sedimentation Rates in an Ionic Liquid. *J. Phys. Chem. Lett.* **2011**, *1*, 64–68.
- (13) Clark, S. C.; Walz, J. Y.; Ducker, W. A. Atomic Force Microscopy Colloid–Probe Measurements with Explicit Measurement of Particle–Solid Separation. *Langmuir* **2004**, *20*, 7616–7622.
- (14) Chan, D. Y. C.; Dagastine, R. R.; White, L. R. Forces between a Rigid Probe Particle and a Liquid Interface, I. The Repulsive Case. *J. Colloid Interface Sci.* **2001**, *236*, 141–154.
- (15) Horn, R. G.; Bachmann, D. J.; Connor, J. N.; Miklavcic, S. J. The Effect of Surface and Hydrodynamic Forces on the Shape of a Fluid Drop Approaching a Solid Surface. *J. Phys.: Condens. Matter* **1996**, *8*, 9483–9490.
- (16) Ciunel, K.; Armelin, M.; Findenegg, G. H.; von Klitzing, R. Evidence of Surface Charge at the Air/Water Interface from Thin-Film Studies on Polyelectrolyte-Coated Substrates. *Langmuir* **2005**, *21*, 4790–4793.
- (17) Pawley, J. *Handbook of Biological Confocal Microscopy*; Springer: New York, 2006.
- (18) Nappini, S.; Al Kayal, T.; Norden, B.; Baglioni, P. Magnetically Triggered Release from Giant Unilamellar Vesicles: Visualization by Means of Confocal Microscopy. *J. Phys. Chem. Lett.* **2011**, *2*, 713–718.
- (19) Haupt, B. J.; Pelling, A. E.; Horton, M. A. Integrated Confocal and Scanning Probe Microscopy for Biomedical Research. *Sci. World J.* **2006**, *6*, 1609–1618.
- (20) Pelling, A. E.; Veraitch, F. S.; Chu, C. P.-K.; Mason, C.; Horton, M. A. Mechanical Dynamics of Single Cells during Early Apoptosis. *Cell Motil. Cytoskeleton* **2009**, *66*, 409–422.

(21) Schmidt, S.; Helfer, E.; Carlier, M.-F.; Fery, A. Force Generation of Curved Actin Gels Characterized by Combined AFM-Epi-fluorescence Measurements. *Biophys. J.* **2010**, *98*, 2246–2253.

(22) Tabor, R. F.; Gold, S.; Eastoe, J. Electron Density Matching As a Guide to Surfactant Design. *Langmuir* **2006**, *22*, 963–968.

(23) Manica, R.; Connor, J. N.; Dagastine, R. R.; Carnie, S. L.; Horn, R. G.; Chan, D. Y. C. Hydrodynamic Forces Involving Deformable Interfaces at Nanometer Separations. *Phys. Fluids* **2008**, *20*, 032101/1–032101/12.

(24) Manor, O.; Vakarelski, I. U.; Stevens, G. W.; Grieser, F.; Dagastine, R. R.; Chan, D. Y. C. Dynamic Forces between Bubbles and Surfaces and Hydrodynamic Boundary Conditions. *Langmuir* **2008**, *24*, 11533–11543.

(25) Tabor, R. F.; Manica, R.; Chan, D. Y. C.; Grieser, F.; Dagastine, R. R. Repulsive van der Waals Forces in Soft Matter: Why Bubbles Do Not Stick to Walls. *Phys. Rev. Lett.* **2011**, *106*, 064501/1–063501/4.

(26) Vakarelski, I. U.; Manica, R.; Tang, X.; O'Shea, S. J.; Stevens, G. W.; Grieser, F.; Dagastine, R. R.; Chan, D. Y. C. Dynamic Interactions between Microbubbles in Water. *Proc. Natl. Acad. Sci. U.S.A.* **2010**, *107*, 11177–11182.